Research Article | Vol. 7, No. 6 | 1 Jun 2017 | OPTICAL MATERIALS EXPRESS 2023

Optical Materials EXPRESS

Tunable reflective liquid crystal terahertz waveplates

LEI WANG,[1,2,*] SHIJUN GE,[2] WEI HU,[2] MAKOTO NAKAJIMA,[3] AND YANQING LU[2]

[1]*School of Optoelectronic Engineering, Nanjing University of Posts and Telecommunications, Nanjing 210023, China*
[2]*National Laboratory of Solid State Microstructures, Collaborative Innovation Center of Advanced Microstructures and College of Engineering and Applied Sciences, Nanjing University, Nanjing 210093, China*
[3]*Institute of Laser Engineering, Osaka University, Suita, Osaka 565-0871, Japan*
*wangl@njupt.edu.cn

Abstract: Tunable liquid crystal devices that can change terahertz wave polarization continuously have many potential applications in terahertz optical systems. We present a reflective liquid crystal terahertz waveplate with sub-wavelength metal grating and metal ground plane electrodes. The thickness of the liquid crystal layer can be reduced to ~10% of that needed for the same phase shift at a given frequency in a transmissive waveplate. We experimentally demonstrate the same tunability as in the transmissive type just using half the thickness. We discuss the dependence on the angle of incidence for phase shift tunability, which can achieve beam steering and polarization conversion simultaneously. The proposed design can be applied in terahertz imaging, sensing, and communications.

OCIS codes: (300.6495) Spectroscopy, terahertz; (230.3720) Liquid-crystal devices; (050.5080) Phase shift.

References and links

1. B. Ferguson and X.-C. Zhang, "Materials for terahertz science and technology," Nat. Mater. **1**(1), 26–33 (2002).
2. M. Tonouchi, "Cutting-edge terahertz technology," Nat. Photonics **1**(2), 97–105 (2007).
3. M. Hangyo, "Development and future prospects of terahertz technology," Jpn. J. Appl. Phys. **54**(12), 120101 (2015).
4. A. K. Kaveev, G. I. Kropotov, E. V. Tsygankova, I. A. Tzibizov, S. D. Ganichev, S. N. Danilov, P. Olbrich, C. Zoth, E. G. Kaveeva, A. I. Zhdanov, A. A. Ivanov, R. Z. Deyanov, and B. Redlich, "Terahertz polarization conversion with quartz waveplate sets," Appl. Opt. **52**(4), B60–B69 (2013).
5. S. L. Wadsworth and G. D. Boreman, "Broadband infrared meanderline reflective quarter-wave plate," Opt. Express **19**(11), 10604–10612 (2011).
6. C. Y. Chen, T. R. Tsai, C. L. Pan, and R. P. Pan, "Room temperature terahertz phase shifter based on magnetically controlled birefringence in liquid crystals," Appl. Phys. Lett. **83**(22), 4497–4499 (2003).
7. C. Y. Chen, C. L. Pan, C. F. Hsieh, Y. F. Lin, and R. P. Pan, "Liquid-crystal-based terahertz tunable Lyot filter," Appl. Phys. Lett. **88**(10), 101107 (2006).
8. R. Wilk, N. Vieweg, O. Kopschinski, and M. Koch, "Liquid crystal based electrically switchable Bragg structure for THz waves," Opt. Express **17**(9), 7377–7382 (2009).
9. Y. Wu, X. Ruan, C.-H. Chen, Y. J. Shin, Y. Lee, J. Niu, J. Liu, Y. Chen, K.-L. Yang, X. Zhang, J.-H. Ahn, and H. Yang, "Graphene/liquid crystal based terahertz phase shifters," Opt. Express **21**(18), 21395–21402 (2013).
10. C. F. Hsieh, R. P. Pan, T. T. Tang, H. L. Chen, and C. L. Pan, "Voltage-controlled liquid-crystal terahertz phase shifter and quarter-wave plate," Opt. Lett. **31**(8), 1112–1114 (2006).
11. C. S. Yang, T. T. Tang, P. H. Chen, R.-P. Pan, P. Yu, and C.-L. Pan, "Voltage-controlled liquid-crystal terahertz phase shifter with indium-tin-oxide nanowhiskers as transparent electrodes," Opt. Lett. **39**(8), 2511–2513 (2014).
12. L. Wang, X. W. Lin, W. Hu, G. H. Shao, P. Chen, L. J. Liang, B. B. Jin, P. H. Wu, H. Qian, Y. N. Lu, X. Liang, Z. G. Zheng, and Y. Q. Lu, "Broadband tunable liquid crystal terahertz waveplates driven with porous graphene electrodes," Light Sci. Appl. **4**(2), e253 (2015).
13. G. Isić, B. Vasić, D. C. Zografopoulos, R. Beccherelli, and R. Gajić, "Electrically tunable critically coupled terahertz metamaterial absorber based on nematic liquid crystals," Phys. Rev. Appl. **3**(6), 064007 (2015).
14. D. C. Zografopoulos and R. Beccherelli, "Tunable terahertz fishnet metamaterials based on thin nematic liquid crystal layers for fast switching," Sci. Rep. **5**(1), 13137 (2015).
15. N. Chikhi, M. Lisitskiy, G. Papari, V. Tkachenko, and A. Andreone, "A hybrid tunable THz metadevice using a high birefringence liquid crystal," Sci. Rep. **6**(1), 34536 (2016).

#291271 https://doi.org/10.1364/OME.7.002023
Journal © 2017 Received 29 Mar 2017; revised 28 Apr 2017; accepted 17 May 2017; published 19 May 2017

16. D. Shrekenhamer, W. C. Chen, and W. J. Padilla, “Liquid crystal tunable metamaterial absorber,” Phys. Rev. Lett. **110**(17), 177403 (2013).
17. S. Savo, D. Shrekenhamer, and W. J. Padilla, “Liquid crystal metamaterial absorber spatial light modulator for THz applications,” Adv. Opt. Mater. **2**(3), 275–279 (2014).
18. H. Akiyama, T. Kawara, H. Takada, H. Takatsu, V. Chigrinov, E. Prudnikova, V. Kozenkov, and H. Kwok, “Synthesis and properties of azo dye aligning layers for liquid crystal cells,” Liq. Cryst. **29**(10), 1321–1327 (2002).
19. M. Schadt, H. Seiberle, and A. Schuster, “Optical patterning of multi-domain liquid-crystal displays with wide viewing angles,” Nature **381**(6579), 212–215 (1996).
20. L. Wang, X.-W. Lin, X. Liang, J.-B. Wu, W. Hu, Z.-G. Zheng, B.-B. Jin, Y.-Q. Qin, and Y.-Q. Lu, “Large birefringence liquid crystal material in terahertz range,” Opt. Mater. Express **2**(10), 1314–1319 (2012).
21. X.-W. Lin, J.-B. Wu, W. Hu, Z.-G. Zheng, Z.-J. Wu, G. Zhu, F. Xu, B.-B. Jin, and Y.-Q. Lu, “Self-polarizing terahertz liquid crystal phase shifter,” AIP Adv. **1**(3), 032133 (2011).
22. B. Vasić, D. C. Zografopoulos, G. Isić, R. Beccherelli, and R. Gajić, “Electrically tunable terahertz polarization converter based on overcoupled metal-isolator-metal metamaterials infiltrated with liquid crystals,” Nanotechnology **28**(12), 124002 (2017).
23. S. Slussarenko, A. Murauski, T. Du, V. Chigrinov, L. Marrucci, and E. Santamato, “Tunable liquid crystal q-plates with arbitrary topological charge,” Opt. Express **19**(5), 4085–4090 (2011).
24. B.-Y. Wei, W. Hu, Y. Ming, F. Xu, S. Rubin, J.-G. Wang, V. Chigrinov, and Y.-Q. Lu, “Generating switchable and reconfigurable optical vortices via photopatterning of liquid crystals,” Adv. Mater. **26**(10), 1590–1595 (2014).

1. Introduction

Waveplates are essential and versatile tools for transforming, controlling, or analyzing the polarization state of light. They have widespread applications in modern optical systems; tunable devices that can rotate the polarization continuously are in especially high demand. However, in terahertz (THz) optics [1–3], there are still many challenges. THz polarization conversion with commercial quartz waveplates is mechanically controlled [4]. Mechanically tunable THz reflective waveplates exhibit a dependence on incidence angle and separation distance [5]. However, mechanically tunable devices are bulky and difficult to integrate.

Liquid crystals (LCs) have drawn great attention as promising materials for tunable THz waveplates. In early studies, magnetic fields were used to tune the birefringence of LCs [6, 7]. These devices achieved good tunability, but were bulky, heavy, and highly power-consuming. Many voltage-controlled LC THz waveplates have been developed [8–11]. To achieve the required high phase retardation, large cell gaps (500 μm or more) have been introduced, causing the components to respond very slowly because the decay time of LCs is proportional to the square of the cell gap. In addition, it is quite difficult to implement homogeneous pre-alignment in such thick cells. We have also realized broadband tunable LC THz waveplates driven with porous graphene electrodes [12]. All of these devices operate in the transmission mode. The slow response times and high operation voltages caused by the thick LC layer hamper their further development in practical applications. LC-based metamaterial devices, which rely on resonances, were later invented [13–15]. Their tuning speed is faster due to the small thickness of the LC layer. Although the metamaterials used as electrodes supply a non-uniform static electric field over the LC, the LC is placed in the hot spot of both the terahertz and the low-frequency driving electric field to realize high- performance. If we can supply a uniform static electric field over the LC with metamaterial electrodes, the efficiency and tunable range could be improved further [16, 17].

Herein, combining a sub-wavelength metal grating and a metal ground plane as electrodes, we present an electrically controlled reflective LC THz waveplate. The cell gap can be shortened to just one tenth of that needed in a conventional transmissive waveplate, which can greatly reduce the response time and the voltage required. Additionally, we demonstrate a large phase shift tunable range and the polarization conversion dependence on the angle of incidence is discussed. These properties suggest a compact method to effectively realize electric-driven tunable THz components.

Optical Materials EXPRESS

2. Schematic and principle

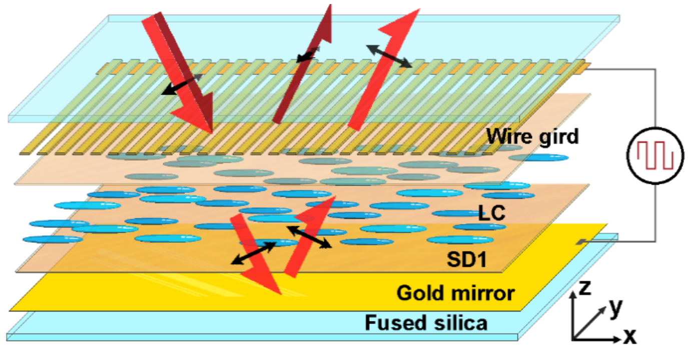

Fig. 1. Schematic drawing of a tunable reflective THz waveplate. The THz component with electric field parallel to the grating is reflected, while the component with perpendicular electric field propagates through the LC layer and is reflected by the gold mirror.

The configuration of the waveplate is illustrated in Fig. 1. It consists of sub-wavelength metal wire grid and metal ground plane that together act as electrodes to control the LC refractive index by voltage. Meanwhile, the electrodes act separately as THz polarizer and mirror. The LC layer fills the gap between the components. Both electrodes are spin coated with sulfonic azo dye (SD1) as an alignment layer and photo-aligned to achieve homogeneity parallel to the grating direction [18, 19]. Therefore, the pre-alignment directions of LC molecules on both substrates are perpendicular to the grating direction. The device is driven by applying a 1 kHz square-wave alternating current signal through copper tapes connecting the electrodes to the electric power source.

The principle of the LC waveplate is quite different from that of the transmissive waveplate, where the ordinary wave and the extraordinary wave both pass through the LC layer. Here, the incident THz wave is decomposed into two linearly polarized components with electric fields parallel and perpendicular to the direction of the grating. The component parallel to the grating is reflected by the wire grid, which is well-known as a polarizer. The other component propagates in the LC layer and is then reflected from the gold mirror. So, a reflective waveplate is obtained by reflecting two components from two different planes. The phase retardation is due to a path length difference between the two orthogonal components of the reflected THz beam. Thus, $\Delta\varphi$ is induced by generating different optical paths for the two THz components, which is presented in Eq. (1). One path is in air and the other is in liquid crystal. Snell's law determines the angle of the THz wave through the LC layer.

$$\Delta\phi = \frac{2\pi}{\lambda}\frac{2h\left(n-\frac{(\sin\theta)^2}{n}\right)}{\cos\left(\sin^{-1}\left(\frac{\sin\theta}{n}\right)\right)} \tag{1}$$

where h is the thickness of LC layer, n is the refractive index of the LC, θ is the incidence angle, and λ is the incident wavelength.

From Eq. (1) we can see that the tunability of the reflective waveplate depends on electrically controlling a nematic liquid crystal. We adjust the direction of the LC by voltage applied between the polarizer and mirror electrodes. The phase of the component propagating through the LC layer is changed due to the varying refractive index of LC. Thus, different phase shifts are produced between the two orthogonal components and tunable THz wave polarization conversion can be realized. Here, we do not take into account the reflection efficiencies and losses of real materials. Compared with the transmissive $\Delta\varphi = 2\pi\ \Delta n\ h/\lambda$, where Δn is due to the LC birefringence, we can see that the reflective $\Delta\varphi$ depends on $2n$, while the transmissive $\Delta\varphi$ depends on Δn. Especially when $\theta = 0°$, the ratio between $\Delta\varphi$ in reflection waveplate and transmission type equal to $2n/\Delta n$. In our LC material, $2n$ is from 3 to 3.6 and Δn is about 0.3 [20]. Therefore, the thickness of LC layer in reflective geometry can be much smaller, about 10% of that in the transmissive one with the same phase shift.

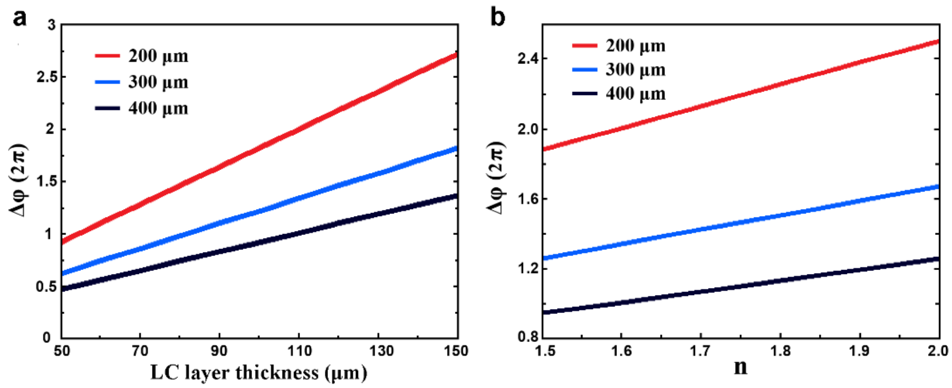

Fig. 2. THz LC waveplate characteristics for different THz wavelengths. (a) Phase difference versus LC layer thickness at n = 1.8. (b) Phase difference versus the LC refractive index at LC layer thickness h = 125 μm.

First, we consider the relationship between phase difference and the LC. Figure 2 shows the results obtained using Eq. (1) at given wavelengths when the incidence angle is zero. We can see that a large phase difference requires a thick LC layer; to obtain the same phase difference for longer wavelengths requires a thicker cell gap. When n = 1.8, the thickness of LC layer is approximately 50 μm for the reflective half-wave plate at 400 μm shown in Fig. 2(a), which is less than 10% of the thickness needed in transmission type.

Figure 2(b) shows that the phase difference increases with the refractive index of LC. LCs with high birefringence have wider tunability. For example, at 1 THz, the refractive index of LC increases from 1.5 to 2.0, and the phase difference can be changed 150° with a layer thickness of 125 μm. The tunability of the reflective LC waveplate is two-fold the tunability of the transmissive waveplate.

3. Experiments

The sub-wavelength gold wire grid polarizer structure is the same as our former sample [21]. It was fabricated through photolithography with 20-μm period and 10-μm linewidth. The Au mirror electrode was grown on silica by CVD with a thickness of 200 nm. Then, photo-sensitive sulfonic azo dye SD1 (Dai-Nippon Ink and Chemicals, Japan) was spin-coated onto the electrodes and photoaligned at 0° to the grating direction. The liquid crystal NJU-LDn-4 [20], with n_0 = 1.5 and Δn = 0.3 in the range 0.5– 2.5 THz, was loaded into the cell by capillary action. The thickness of the LC layer was approximately 125 μm.

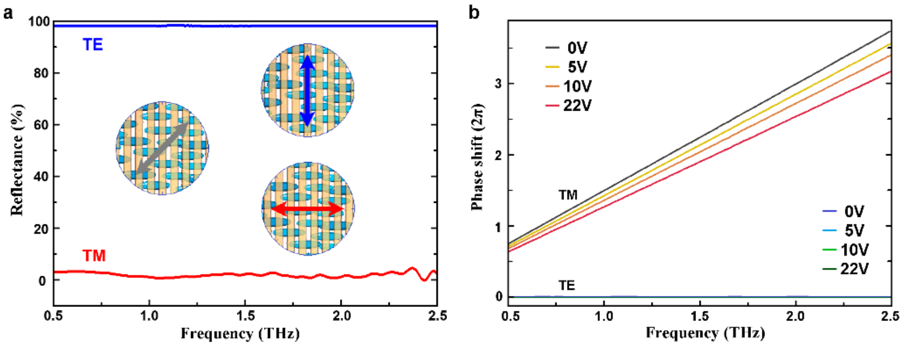

Fig. 3. Frequency- and polarization-dependent characteristics of the THz LC waveplate. (a) Reflectance of the subwavelength gold wire grid; the insets depict the photograph of the Au grating and the polarizations of the THz components. (b). Phase shift at different driving voltages.

A THz time-domain spectroscopy (TDS) system (Advantest TAS7400SP) with reflection geometry was used for measurements. The linearly polarized THz beam was incident at an angle of 11° with the polarization of the electric field oriented at 45° relative to the wire grid. The component parallel to the grid orientation (TE mode) was reflected by the grating, while the perpendicular (TM mode) component was transmitted. We can see from Fig. 3(a) that TE reflectance is nearly 100% and TM reflectance is nearly 0 over the range 0.5–2.5 THz. Figure 3(b) displays the voltage-dependent phase shift of the two components determined by applying a 1-kHz square-wave AC signal to the LC cell. The phase of the reflected TE does not change, so the phase shift is zero compared to the reference. The phase shift of the TM mode transmitted through the LC layer decreases as operating voltage increases. The maximum phase difference between the two modes occurs at 0 V. The saturation voltage of the sample is 22 V. At 0.5 THz, the phase shift reaches about 1.2π while in transmissive LC THz waveplate with double thickness of LC layer, the phase shift is just about 0.2π [12], which show reasonable agreement for the theoretical analysis.

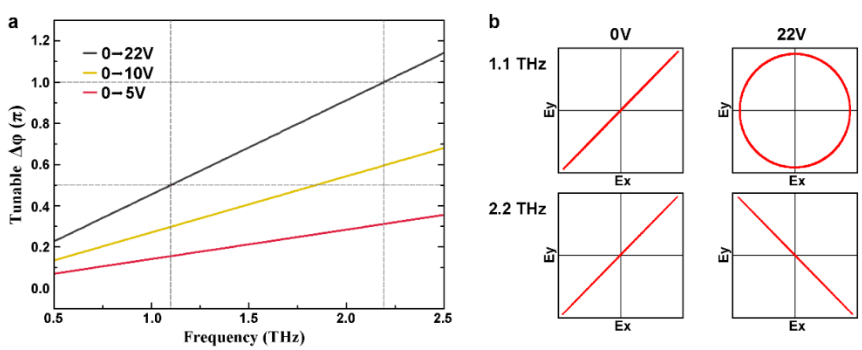

Fig. 4. Electrically tunable characteristics of the THz LC waveplate. (a) Tunability of phase difference for different voltage ranges. (b) Polarization evolution (0–22 V) from linearly polarized to circularly polarized at 1.1 THz, to orthogonally linearly polarized at 2.2 THz.

The extracted tunable phase difference is shown in Fig. 4(a). It has a nearly linear response to wavelength over the operating voltage range. The phase retardation becomes larger as applied voltage increases. We can see the evolution of the polarization by tuning the operation voltage, which is comparatively low. We select 1.1 THz and 2.2 THz to test the polarization conversion, as shown in Fig. 4(b). The polarization can be changed from linear to circular polarization at 1.1 THz, while an orthogonal linear polarization is obtained at 2.2 THz by tuning the applied voltage from 0 V to 22 V. So, by electrically tuning the LC, the

Optical Materials EXPRESS

operation frequency of the tunable quarter-wave plate can cover the range 1.1–2.5 THz, and that of the tunable half-wave plate is 2.2–2.5 THz. The same tunability as in transmissive type just using half the thickness is realized [12]. These results are not strictly in agreement with Eq. (1), mainly because the cell gap inhomogeneity and multiple reflections are not considered.

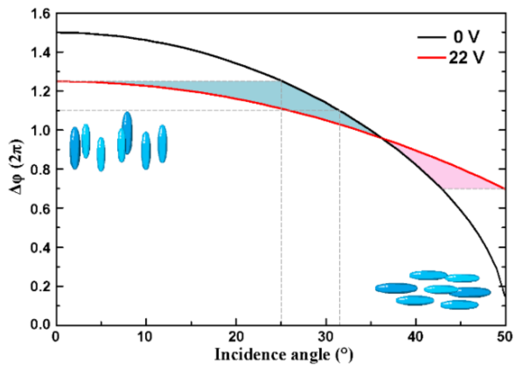

Fig. 5. Dependence of phase difference on angle of incidence for the THz LC waveplate at two voltages of interest.

4. Discussion

Although we are limited by the experimental system, there is a potential for tuning the phase difference by varying the incident angle of the THz beam according to Eq. (1). Combined with the LC refractive index [Eq. (2)], the phase difference decreases as the incident angle increases, as indicated in Fig. 5. The operation frequency is 1 THz.

$$n_{eff}^2 = \frac{n_e^2 n_o^2}{n_e^2 \cos^2 \alpha + n_o^2 \sin^2 \alpha} \tag{2}$$

where α is the angle between the optical axis and the direction of light propagation, n_o is ordinary refractive index, and n_e is extraordinary refractive index.

We can realize the same polarization conversion at different directions. During increasing the angle of incidence period, there is a crossing point at about 35° of the two different operation voltage situations. Before 35°, the phase difference at 0 V is larger than that at 22 V, decreasing the operating voltage can compensate for the decrease of the phase difference induced by the incident angle increase. When the incident angle of THz wave is larger than 35°, increasing the operating voltage can compensate for the decrease of the phase difference. Based on our simple analysis, to some extent, it can realize beam steering for a given polarization conversion in a certain range.

Although we focus on the tunable phase shift, if the LC losses of our proposed device are considered, there are at least two ways to compensate the different absorption loss between the two mode components. One is to control the polarization of the incident THz wave to make the TM component larger than the TE component in order to compensate for the loss of the TM component as it propagates through the LC layer. The other is to stack the same LC cell except for the graphene layer used as THz transparent electrode [12]. Furthermore, the performance of tunability may be enhanced by stacking LC cells.

Although, we use sub-wavelength metal grating as polarizer electrode, which can also be considered as a type of metamaterial, we don't exploit the resonant property of metamaterial to control the phase shift. LC tunable THz metamaterial devices have fast response time and low operating voltage with much lower thickness of the LC layer [22]. Integrating our waveplate into metamaterial may have many potential applications.

Optical Materials EXPRESS

5. Conclusions

We have proposed and demonstrated an electrically tunable reflective THz waveplate based on a thin LC layer with sub-wavelength metal wire grid and metal mirror electrodes. The compact device can rapidly change the polarization continuously with low operation voltages compared to transmissive THz waveplates. Polarization evolution as a quarter- or half-waveplate can also be realized for different frequency ranges. In addition, the incidence angle tunability of the reflective waveplate was studied. Beam steering and polarization conversion can be obtained simultaneously by rotating the waveplate and tuning voltage at the same time. Based on a similar strategy, the development of various high-performance tunable THz components for amplitude, phase, and complex wavefront control, such as Q-plates [23] and vortex beam generators [24], can be expected to serve an important role in THz imaging, sensing, and security applications.

Funding

National Natural Science Foundation of China (No. 61605088); Natural Science Foundation of Jiangsu Province (No. BK20150845,15KJB140004); Open Foundation Project of National Laboratory of Solid State Microstructures (M28003); China Scholarship Council (CSC); Research Center of Optical Communications Engineering and Technology, Jiangsu Province.

Acknowledgments

The authors would like to thank V. Chigrinov for his kind support with the photoalignment technique and Hao Qian for his assistance in drawing the schemes, and China Scholarship Council for financial support.